

Solvolysis Mechanisms of RNA Phosphodiester Analogues Promoted by Mononuclear Zinc(II) Complexes: Mechanistic Determination upon Solvent Medium and Ligand Effects

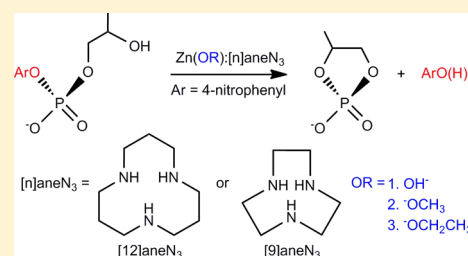
Xuepeng Zhang,[†] Yajie Zhu,[†] Hui Gao,[‡] and Cunyuan Zhao^{*†}

[†]MOE Key Laboratory of Bioinorganic and Synthetic Chemistry, School of Chemistry and Chemical Engineering, Sun Yat-Sen University, Guangzhou 510275, P. R. China

[‡]Key Laboratory of Renewable Energy and Gas Hydrate, Guangzhou Institute of Energy Conversion, Chinese Academy of Sciences, Guangzhou 510640, P. R. China

S Supporting Information

ABSTRACT: The solvolysis mechanisms of RNA phosphodiester model 2-(hydroxypropyl)-4-nitrophenyl phosphate (HpPnP) catalyzed by mononuclear zinc(II) complexes are investigated in the paper via a theoretical approach. The general-base-catalyzed (GBC) and specific-base-catalyzed (SBC) mechanisms are thoroughly discussed in the paper, and the calculations indicate a SBC mechanism (also named as the direct nucleophilic attack mechanism) when the cyclization of HpPnP is promoted by the Zn:[12]aneN₃ complex ([12]aneN₃ = 1,5,9-triazacyclododecane). The ligand effect is considered by involving two different catalysts, and the results show that the increasing size catalyst provides a lower energy barrier and a significant mechanistic preference to the SBC mechanism. The solvent medium effect is also explored, and reduced polarity/dielectric constant solvents, such as light alcohols methanol and ethanol, are more favorable. Ethanol is proven to be a good solvent medium because of its low dielectric constant. The computational results are indicative of concerted pathways. Our theoretical results are consistent with and well interpret the experimental observations and, more importantly, provide practical suggestions on the catalyst design and selection of reaction conditions.

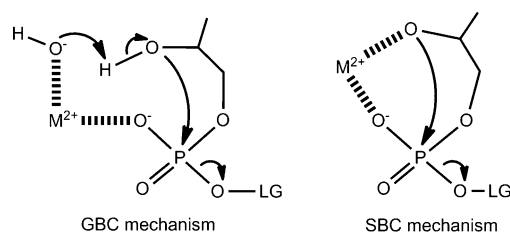


INTRODUCTION

Phosphate esters are ubiquitous in organisms and play vital roles in a host of biochemical processes.¹ DNA and RNA are phosphate diesters, and their solvolysis cleavage of P–O bonds promoted by either natural enzymes or artificial chemical mimic arouse continual interest and are the subject of some comprehensive reviews.² Exceptional kinetic stability of P–O bonds in DNA against hydrolysis in a neutral aqueous solution is observed,³ while the phosphodiester bonds in RNA can be hydrolyzed much more readily under identical conditions because of the presence of 2'-OH ion on the ribose ring.⁴ Their kinetic stability makes DNA and RNA particularly suitable for their biological roles in which high resistance to hydrolysis is a prerequisite for DNA to store genetic codes and relatively easier cleavage is necessary for RNA, i.e., message RNA, for instance, which requires rapid hydrolysis after mission accomplished. However, the significant repulsion between the electronegative phosphate backbone of RNA and potential nucleophilic agents hinders spontaneous hydrolysis in the absence of catalysts.¹ Although plenty of natural enzymes and various chemical mimics, especially metal complexes are utilized to cleave the P–O bonds of RNA, there is still no universal mechanism for RNA hydrolysis issues.^{2u} Practical suggestions on the catalyst design and insightful guidelines for mechanistic determination should be drawn from more specific conditions.

There has been a hot debate on general-base-catalyzed (GBC) or specific-base-catalyzed (SBC, also named as the nucleophilic mechanism⁵) mechanisms on solvolysis cleavage of phosphate diesters promoted by some metal complexes (Scheme 1).⁶ The rate constant is generally proportional to the concentrations of all bases or some specific lyoxides in the GBC and SBC mechanisms, respectively. The GBC mechanism is usually accepted for the hydrolysis of RNA dinucleotide analogues, such as 2-(hydroxypropyl)-*p*-nitrophenyl phosphate (HpPnP), involving participation of the metal-bound lyoxide, which acts as a general base to facilitate deprotonation of a

Scheme 1. Schematic Depiction Presented for the GBC and SBC Mechanisms



Received: May 9, 2014

Published: October 31, 2014

solvent molecule, and both nucleophilic attack and proton transfer occur in the rate-limiting step.^{6g,i,7} Alternatively, the SBC mechanism is proposed in some reactions,^{6e,f,i,8} in which proton transfer is involved in a preequilibrium step and nucleophilic attack occurs in the rate-determining step. The classical experimental approach to distinguish the GBC mechanism from the SBC mechanism is the solvent deuterium isotope effect (Dk). The Dk value obtained below 1.5 usually indicates that no proton is in flight in the rate-determining step and is diagnostic of a SBC mechanism, while a Dk value larger than 2.0 indicates a GBC mechanism.⁹ It should be noted that most of the previous experimental studies, particularly those reported by Richard, Morrow, and co-workers,^{6a,10} and Williams and collaborators,^{6f,11} indicate a SBC mechanism. However, Brown and co-workers,^{6i,12} on the basis of the solvent deuterium isotope effect and kinetic consideration, point to a GBC concerted mechanism for the reaction when light alcohols, such as methanol and ethanol, are solvent media. However, it is usually not sufficient enough to conclude reaction mechanisms via merely experimental approaches. A combination of theoretical and experimental efforts is more convincing and insightful. Despite the large number of experimental investigations, theoretical approaches of the reaction are rare.^{6e,g,i,13} Most previous calculation results reported by Brown and co-workers utilizing bimetallic complexes,^{6f} by Fan and Gao involving monozinc complexes,^{6g} and by Mancin and collaborators using mononuclear zinc(II) complexes¹³ are indicative of a GBC mechanism. Alternately, the SBC mechanism is found to be favorable in our previous work utilizing a binuclear zinc(II) complex to promote transesterification of the RNA analogue HpPNP.^{6e}

It is also pointed out that the active sites of enzymes comprise dominant reduced dielectric constant entities and prefer a low dielectric constant/polarity environment.¹⁴ Recently, the medium effect was systematically investigated by Brown and co-workers using several zinc(II) complexes to cleave the phosphodiester P–O bonds in various solvent media, such as water and light alcohols.^{6i,12,15} They found that a better rate acceleration was observed in a reduced dielectric constant solvent medium. However, detailed mechanistic descriptions of concerted or stepwise mechanisms (GBC or SBC), especially considering the solvent medium effect, are still less explicit.

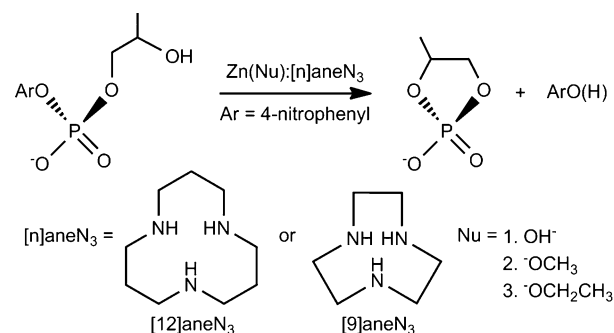
The criteria of labile metal ions frequently employed in synthetic hydrolases are concluded as follows: (1) a harder Lewis acid for binding to hard oxygen/nitrogen anions of the electronegative phosphodiester backbone of nucleic acids; (2) a stronger Lewis acid for polarizing phosphoryl bonds to activate the substrate; (3) rapid ligand exchange; (4) redox inertness (not required) to rule out competing oxidative cleavage, which is very efficient but less controllable. Zinc(II) ions are therefore more preferred: higher charge density (2.7 \AA^{-1}) to be a harder Lewis acid, higher ionization potential (17.96 eV) to be a stronger Lewis acid, and higher rate constant for the substitution of water on the aquo ions ($10^{7.4} \text{ s}^{-1}$).^{2c} More importantly, zinc(II) ions have a filled 3d shell and the resultant ligand-field stabilization energy is not considered, which enable zinc(II) complexes to change their geometries without energetic barriers.

Solvolysis cleavage of RNA dinucleotide analogues promoted by mononuclear zinc(II) complexes has been extensively investigated in the past decades. Kimura and co-workers found that the tridentate complex $\text{Zn}:[12]\text{aneN}_3$ ($[12]\text{aneN}_3 = 1,5,9\text{-triazacyclododecane}$) was more catalytically effective than

the tetradentate complex $\text{Zn}:[12]\text{aneN}_4$ ($[12]\text{aneN}_4 = 1,4,7,10\text{-tetraazacyclododecane}$).¹⁶ Mancin and co-workers investigated the ligand effect via the use of a series of increasing size macrocyclic amine ligands, such as $[9]\text{aneN}_3$ (1,4,7-triazacyclononane) and $[12]\text{aneN}_3$.⁵ Chin and co-workers utilized a series of cobalt(III) complexes to explore the structure–reactivity relationship and found that the increasing size ligands are beneficial to the catalytical power.¹⁷ However, a direct mechanistic comparison on the ligand effect is not provided in their experimental works. Hence, it is meaningful and necessary to explore these issues by a theoretical approach.

In the paper, solvolysis cleavage of the RNA dinucleotide analogue HpPNP promoted by two mononuclear zinc(II) complexes, $\text{Zn}:[12]\text{aneN}_3$ and $\text{Zn}:[9]\text{aneN}_3$, is investigated, aiming to provide a detailed mechanistic description considering the solvent medium and ligand effects (Scheme 2).

Scheme 2. Reactions Catalyzed by Two Mononuclear Zinc(II) Complexes with HpPNP as the Substrate and Water and Light Alcohols as the Solvent Media



EXPERIMENTAL SECTION

The *Gaussian 09* program¹⁸ was utilized to perform all of the calculations using density functional theory (DFT). As applied in our previous work,^{6e,19} the hybrid B3LYP²⁰ exchange–correlation functional is proven to be sufficient enough to describe the phosphate transesterification issues and, more importantly, at a lower computational expense. To test the reliability of the B3LYP functionals, the BHandHLYP^{20b,21} functionals were also employed at the same computational level. The results obtained from both the B3LYP and BHandHLYP functionals are qualitatively similar to each other and well consistent with experimental observations (Table S1 in the Supporting Information, SI). Hence, all reported structures in the paper were fully optimized using the most popular hybrid B3LYP functionals. The Stuttgart/Dresden basis sets with effective core potential²² were used for zinc atoms, and diffusion functional basis sets 6-31+G(d,p) were employed for other light atoms, considering highly polarized P–O bonds and corresponding highly charged phosphorus and oxygen atoms during the reaction. Frequency calculations on optimized structures were performed to obtain thermodynamic data and to distinguish transition states from local minima. All transition states were reconfirmed by employing an intrinsic reaction coordinate (IRC) method.²³ The solvation energies for all optimized structures in solution were estimated by employing the polarized continuum model²⁴ with SMD²⁵ single-point calculations. All of the thermodynamic data were obtained at 298.15 K.

RESULTS AND DISCUSSION

For simplicity, the key structural data of the optimized reaction structures in the proposed mechanisms are provided in Table S2 in the SI. Phosphoryl transfer would appear to be a simple nucleophile displacement reaction. However, this simplicity is

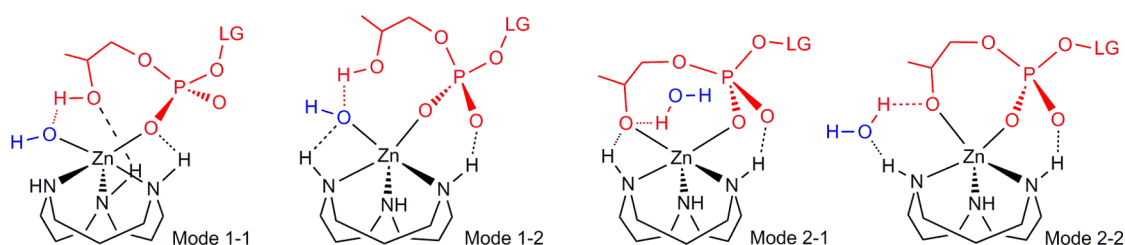
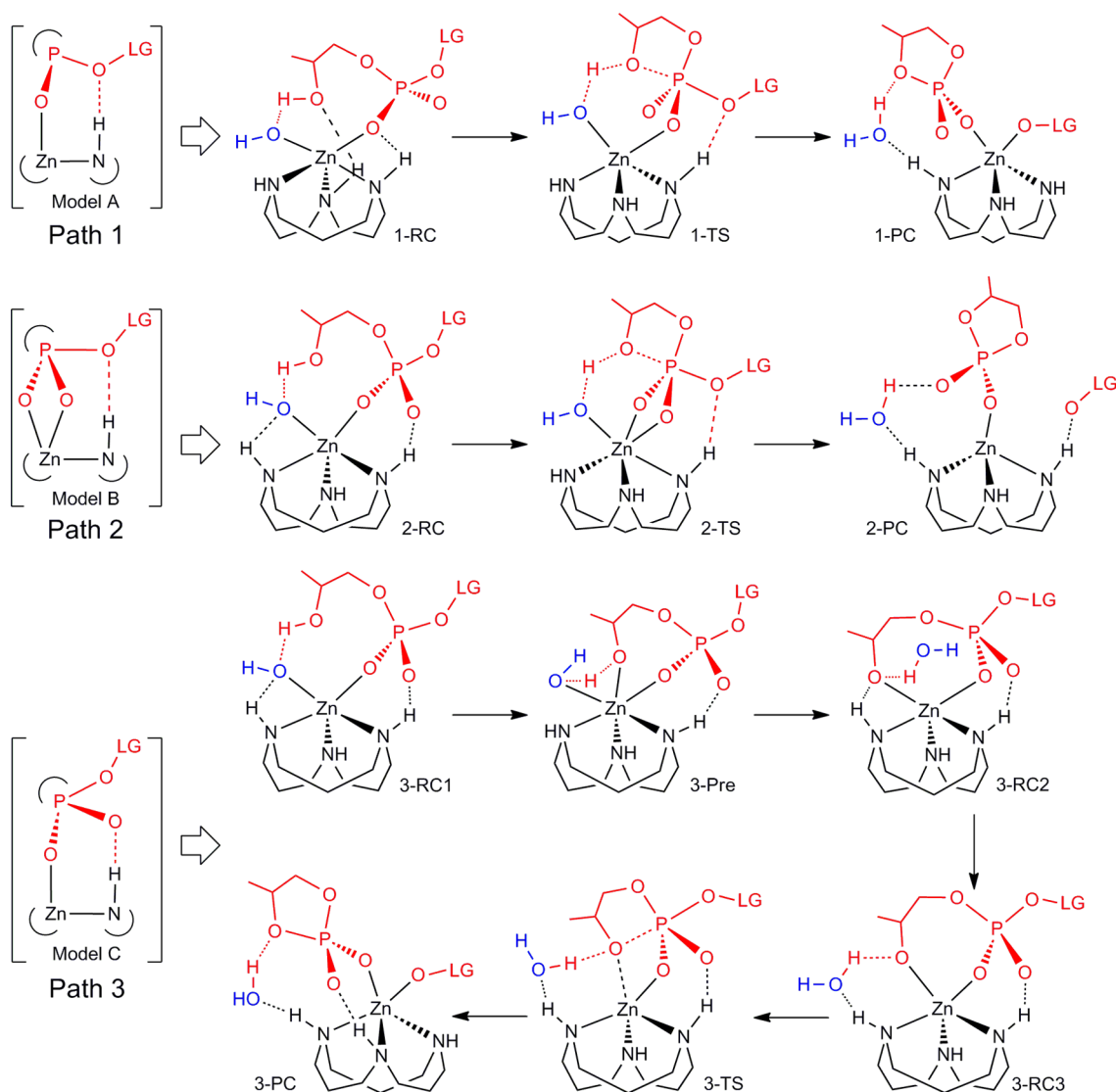


Figure 1. Possible binding modes of the catalyst-substrate complexes.

Scheme 3. Schematic Representations of the Proposed Mechanisms of the Cyclization of HpPNP Promoted by Zn(OH): [12]aneN₃



deceptive, even promoted by a simple mononuclear metal complex. A bimolecular process in metal complexes with macrocyclic triamine ligands can be observed in some specific conditions,^{15d,f,26} but others are usually not. In the paper, dimerization of mononuclear zinc(II) complexes is not considered in order to keep our calculations more tractable and concentrate more on mechanistic determination by the solvent medium and ligand effects. The metal-coordinated ROH is acidic, and the state of ionization depends on the pK_a and pH of the reaction. The pK_a values for the metal-coordinated water molecule in Zn(H₂O):[9]aneN₃ and Zn-

(H₂O):[12]aneN₃ are 8.1 and 7.4, respectively.⁵ Deprotonation of a metal-coordinated alcohol is also evaluated, and the pK_a values for zinc-coordinated ROH in Zn(ROH):[12]aneN₃ are 9.2 in methanol and 7.5 in ethanol.^{15a,27} It is well acknowledged that fully protonated catalysts are catalytically inactive, while their deprotonated counterparts are more competitive and are active catalysts. Meanwhile, the [RO⁻]/[Zn:[12]aneN₃] ratio increases with a rise of the pH of the reaction. Therefore, the pH values of the reactions are larger than the corresponding pK_a values in order to facilitate deprotonation of the metal-coordinated ROH molecules and make the [RO⁻]/[Zn:

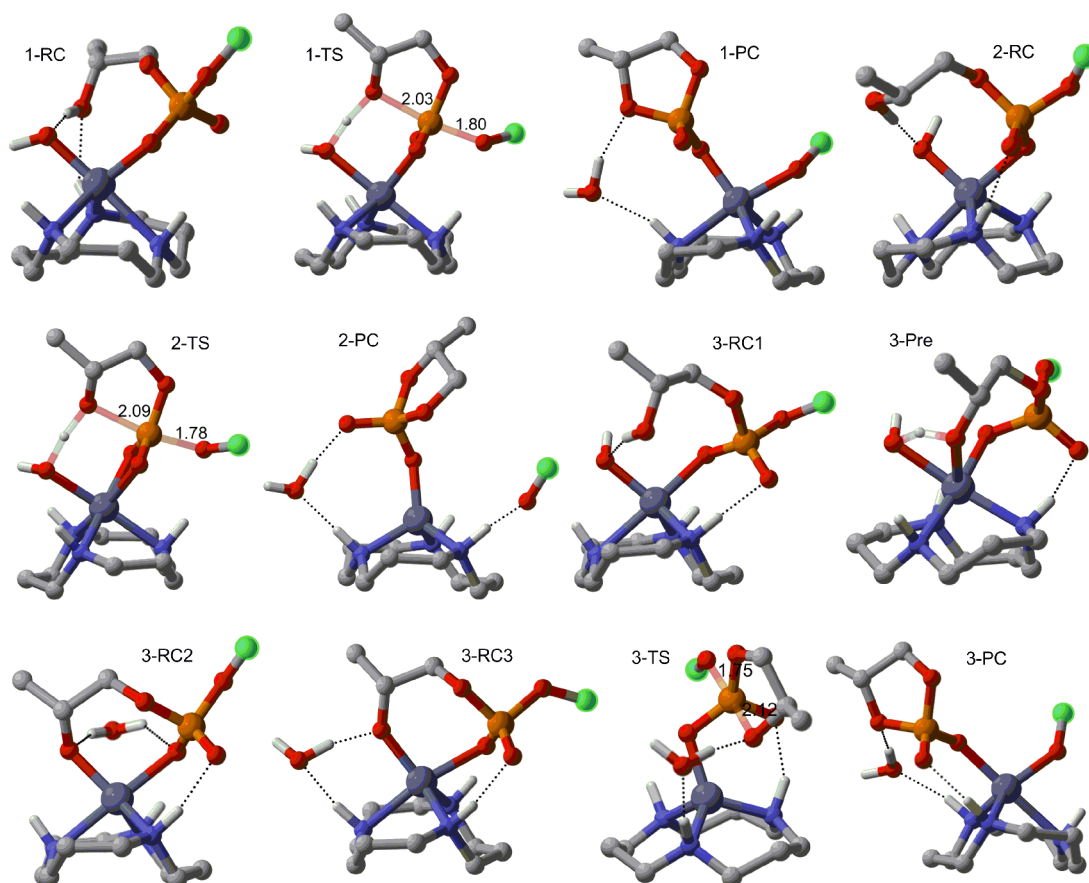


Figure 2. Optimized structures (in water) in the proposed paths 1–3. All carbon-bound hydrogen atoms and the leaving groups (linked to the highlighted carbon atom) are omitted for clarity. Key bond distances in the transition states are presented in angstroms.

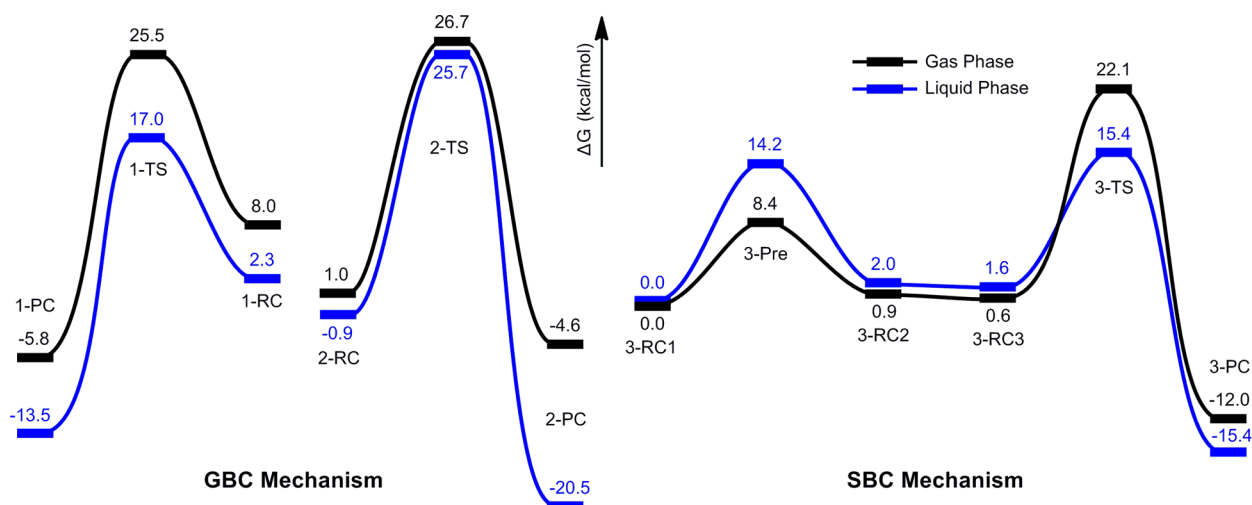


Figure 3. Relative free energy profiles of reaction structures (in water) in the proposed paths 1–3 of the cyclization of HpPnP promoted by Zn(OH):[12]aneN₃.

[12]aneN₃] ratio larger than 0.5.^{5,15c,f} Thereby, only the basic form Zn(RO⁻):[12]aneN₃ is considered in the paper.

Coordination and Binding Modes. The tridentate complex Zn:[12]aneN₃ or Zn:[9]aneN₃ provides two cis-oriented labile sites to bind both the substrate and a hydroxide ion in aqueous solution or an alkoxy group in alcohols.^{2c} In the reactant complex, a Zn–O coordination bond is formed between the metal center and a phosphoryl oxygen atom in the substrate. The other available binding site of the metal center

could be occupied by either a lyoxide or the pendant hydroxypropyl from the substrate. Meanwhile, previous studies have shown that the pK_a values for water molecules and alcoholic hydroxy groups when coordinated with metal centers are almost identical.²⁸ Significant hydrogen bonds are found to stabilize the catalyst–substrate complexes. In this study, four different catalyst–substrate binding modes are considered (Figure 1). For simplicity's sake, only the Zn(OH):[12]aneN₃ case is provided in Figure 1. The fifth binding site

of the metal center is coordinated with either a hydroxide ion in separate modes 1-1 and 1-2 or the pendant isopropoxyl moiety in modes 2-1 and 2-2, respectively. Two significant hydrogen bonds between macrocyclic triamines and the substrate are generated in each provided mode. Both hydrogen bonds help to stabilize the substrate in modes 1-1 and 2-1, while one hydrogen bond plays an important role in stabilizing the hydroxide ion in separate modes 1-2 and 2-2. The free energies of the four provided catalyst–substrate binding modes are quantitatively close, and fast equilibria could occur, which will be discussed in the ensuing chapters or paragraphs.

Mechanisms for the Cyclization of HpPNP Promoted by Zn:[12]aneN₃ in Aqueous Solution and Alcohols.

Basic Reaction Mechanisms. The proposed mechanisms, optimized structures, and their relative free energy surface profiles are presented in Scheme 3 and Figures 2 and 3, respectively. Three reaction pathways are proposed, and both paths 1 and 2 are GBC mechanisms while path 3 adopts the SBC mechanism. The reactant complex 1-RC is constructed according to mode 1-1 of the catalyst–substrate binding modes, in which two mild hydrogen bonds are formed between the substrate and macrocyclic triamines of the catalyst. In 1-RC, a significant hydrogen bond also exists between the metal-coordinated hydroxide ion and the pendant hydroxypropyl from the substrate. Subsequently, the metal-coordinated hydroxide ion acts as a general base to facilitate deprotonation of the nucleophile alcoholic hydroxy group, simultaneous with nucleophilic attack on the positive phosphorus center of the substrate by the to-be-deprotonated hydroxypropyl group, and thereby transition state 1-TS is obtained. Both P–O bond formation to the nucleophile and bond fission to the leaving group (*p*-nitrophenyl) are observed in 1-TS, and finally the leaving group is dissociated to the catalyst in 1-PC. In conclusion, both proton transfer and nucleophilic attack are observed in the rate-limiting step, and thereby path 1 is a concerted GBC mechanism. 2-RC is obtained according to mode 1-2, in which the pendant hydroxypropyl group is stabilized by a hydrogen bond from the metal-coordinated hydroxide ion. In 2-RC, one phosphoryl oxygen is coordinated with the metal center and the other one is stabilized by a significant hydrogen bond. The mechanisms of nucleophilic attack and proton transfer in 2-TS are similar to those of 1-TS, and path 2 is also a concerted GBC mechanism. It should be noted that both phosphoryl oxygen atoms are coordinated with the metal center and form a Zn–O–P–O four-membered ring in 2-TS.

Path 3 is a SBC mechanism, and the potential reactant complexes are proposed as 3-RC1 (based on mode 1-2), 3-RC2 (based on mode 2-1), and 3-RC3 (based on mode 2-2). A quick equilibrium exists between 3-RC1 and 3-RC2, in which the metal-coordinated hydroxide ion acts as a general base to facilitate deprotonation of the pendant hydroxypropyl group of the substrate. A quick mutual exchange occurs between 3-RC2 and 3-RC3 via the rearrangement with a negligible energetic barrier. In 3-RC3, the two cis-oriented labile sites of the metal center are occupied by the substrate: one Zn–O(P) coordination bond in combination with a (N)H–O(P) hydrogen bond helps to activate the substrate via Lewis-acid-induced bond polarization, while the other Zn–O(C) coordination linkage brings the nucleophile isopropoxy in close proximity to the electron-deficient phosphorus center. Subsequently, nucleophilic attack happens in the transition state 3-TS, and finally the cyclic phosphate and 4-nitrophenyl

are obtained in the transient product 3-PC. In conclusion, path 3 involves three potential reactant complexes, proton transfer happens in a preequilibrium step, and nucleophilic attack is the rate-limiting step.

Inspection of the relative free energy profiles (Figure 3) shows that path 3 is the most favored mechanism among the three proposed reaction pathways and the SBC mechanism is more favorable than the GBC mechanism in the condition. The sum of the relative free energies of the dissociative Zn(OH[−]):[12]aneN₃ and HpPNP is considered to obtain the overall free energy barrier. The estimation of free energies of bimolecular processes tends to be inaccurate because of the overestimation of the entropic contributions of the translational and rotational terms, which are highly suppressed by the bulk solvent. Therefore, a corrected free energy is calculated by the equation provided below. The *f* and *f'* factors are within 0 to 1. When *f* = *f'* = 1, the entropic contributions of the translational and rotational movements are totally considered and the sum of the relative free energies of the starting materials (the dissociative Zn(OH[−]):[12]aneN₃ and HpPNP) is −16.2 kcal/mol. The relative free energy value turns out to be 4.4 kcal/mol when the contributions of the translational and rotational movements are completely not considered. In fact, the sum of the relative free energies of the starting materials is a compromise value, between −16.2 and +4.4 kcal/mol. The *f* and *f'* factors are estimated to be small (<0.5) because of the fact that the translational and rotational movements are highly suppressed by the bulk solvent. In the paper, the *f* and *f'* factors are given in 0.3–0.4, and the sum of the relative free energies of the starting materials is −1.8 to −3.8 kcal/mol. Therefore, the overall free energy barrier of path 3 is 17.2–19.2 kcal/mol and is in good agreement with the experimental result (19.8 kcal/mol, calculated from the observed second-order rate constant reported for the reaction in water of $1.8 \times 10^{-2} \text{ M}^{-1} \text{ s}^{-1}$).⁵

$$\Delta G_{\text{corr}} = \Delta H - T(\Delta S_{\text{elec}} + \Delta S_{\text{vib}} + f\Delta S_{\text{trans}} + f'\Delta S_{\text{rot}})$$

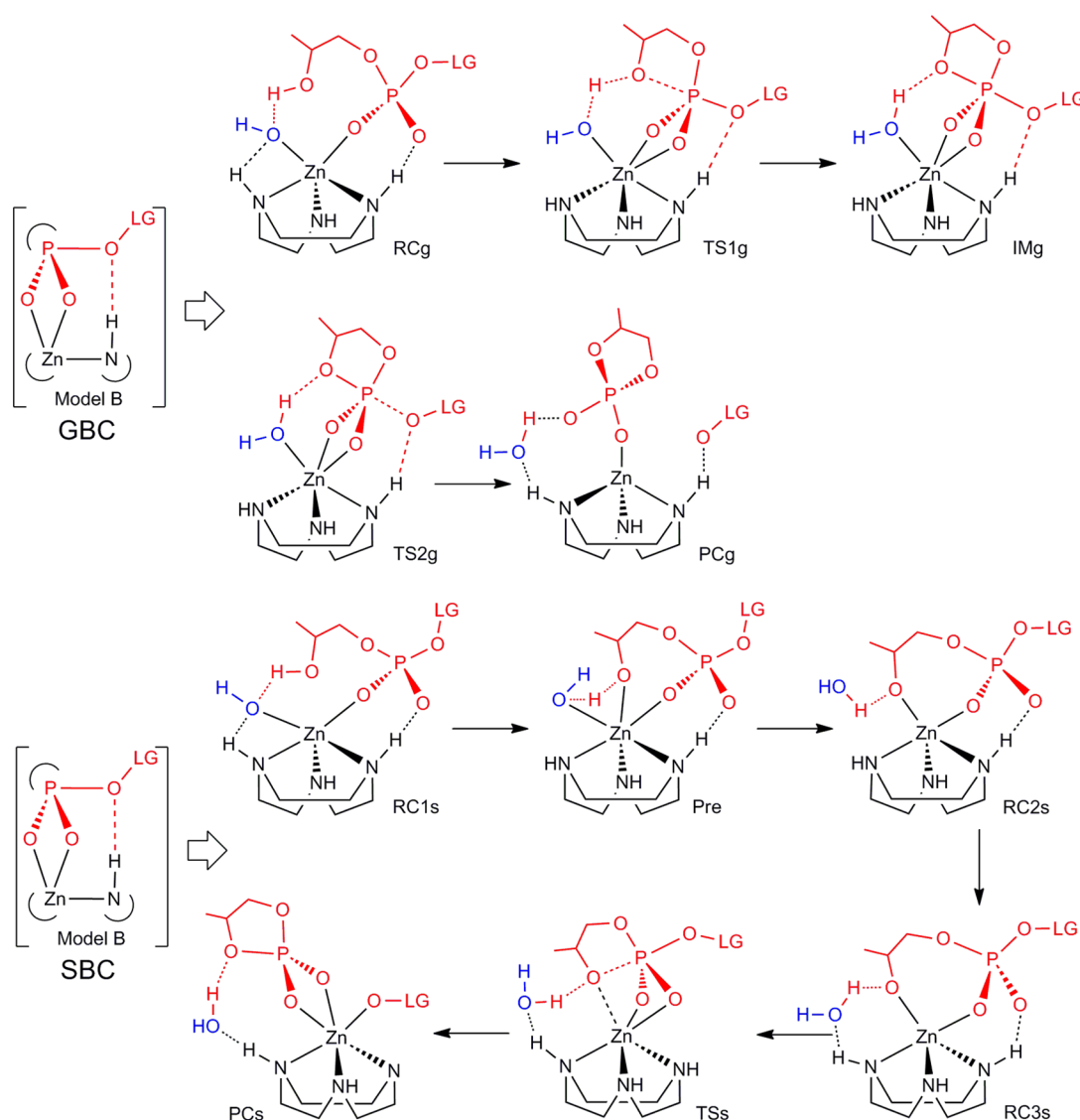
More details can be discerned from the combination of Scheme 3 and Figures 2 and 3. 3-RC1 is more stable than 1-RC, which indicates that the hydrogen bonds are more inclined to occur between the macrocyclic triamines and phosphoryl oxygen atoms from the substrate. This kind of hydrogen-bond network helps to better recognize and stabilize the substrate. The same coincidences can be seen in the rate-determining transition states (seen in Scheme 3). The (N)H–O(P) hydrogen bonds in models A (adopted in path 1) and B (utilized in path 2) are designed to stabilize the leaving group, while that in model C (adopted in path 3) plays a significant role in stabilizing the phosphorane-like transition state. Therefore, it can be concluded that it is more important and favorable for amine-bound hydrogen bonds to stabilize the transition states than to stabilize the leaving group. Model B is assumed to be less favored because of a strained four-membered [Zn(O₂)P] ring.

Solvent Medium Effect. In reference to Figure 3, path 2 is obviously less favorable and, consequently, the mechanistic analogues of paths 1 and 3 are only considered in alcohols in order to keep the calculations more tractable for our computational resources. Significant mechanistic similarities are found between the aqueous solution and reduced polarity/dielectric constant alcohols. For simplicity's sake, the GBC and SBC mechanisms obtained from alcoholic medium are still nominated as paths 1 and 3, respectively. The relative free

Table 1. Relative Free Energies (in kcal/mol) of the Reaction Species in Aqueous Solution and in Reduced Polarity Alcohols

medium ^a	phase	1-RC	1-TS	1-PC	3-RC1	3-Pre	3-RC2	3-RC3	3-TS	3-PC
water	gas	8.0	25.5	-5.8	0.0	8.4	0.9	0.6	22.1	-12.0
	liquid	2.3	17.0	-13.5	0.0	14.2	2.0	1.6	15.4	-15.4
methanol	gas	3.0	24.1	-8.8	0.0	6.5	-1.7	-1.6	19.4	-16.2
	liquid	1.3	15.1	-16.2	0.0	11.7	-1.5	-0.5	13.2	-19.6
ethanol	gas	8.9	24.1	-9.1	0.0	6.5	-1.1	-2.2	18.5	-17.0
	liquid	5.6	16.2	-16.8	0.0	11.7	-1.0	-1.7	12.5	-20.6

^aThe gas- and liquid-phase free energies quoted are for the hydroxy (in the row of water), methoxy (in the row of methanol), and ethoxy (in the row of ethanol) involved complexes, respectively.

Scheme 4. Schematic Representations of the Proposed Mechanisms of the Cyclization of HpPNP Promoted by Zn(OH): [9]aneN₃ in Aqueous Solution

energies of the reaction structures in alcohols are presented in Table 1.

Inspection of Table 1 shows that (1) the relative free energy barriers in path 1 in aqueous solution and in alcohols are higher than their counterparts in path 3 (17.0 vs 15.4 in aqueous solution, 15.1 vs 13.2 in methanol, and 16.2 vs 12.5 in ethanol), which indicates that the SBC mechanism is more favorable than the GBC mechanism considering the solvent medium effect. However, the energy barrier differences between the two

mechanisms in aqueous solution (1.6 kcal/mol) and methanol (1.9 kcal/mol) are too small to be exclusive, (2) the relative free energy barrier of either path 1 or 3 decreases with the descending polarity/dielectric constant of the solvent medium, which implies that the reduced polarity solvents, such as methanol and ethanol, are better options for solvolysis cleavage of phosphate esters. Our calculated results are in agreement with the experimental observations of Brown and coauthors' work^{15e,f} except the failure of mechanistic predictions in light

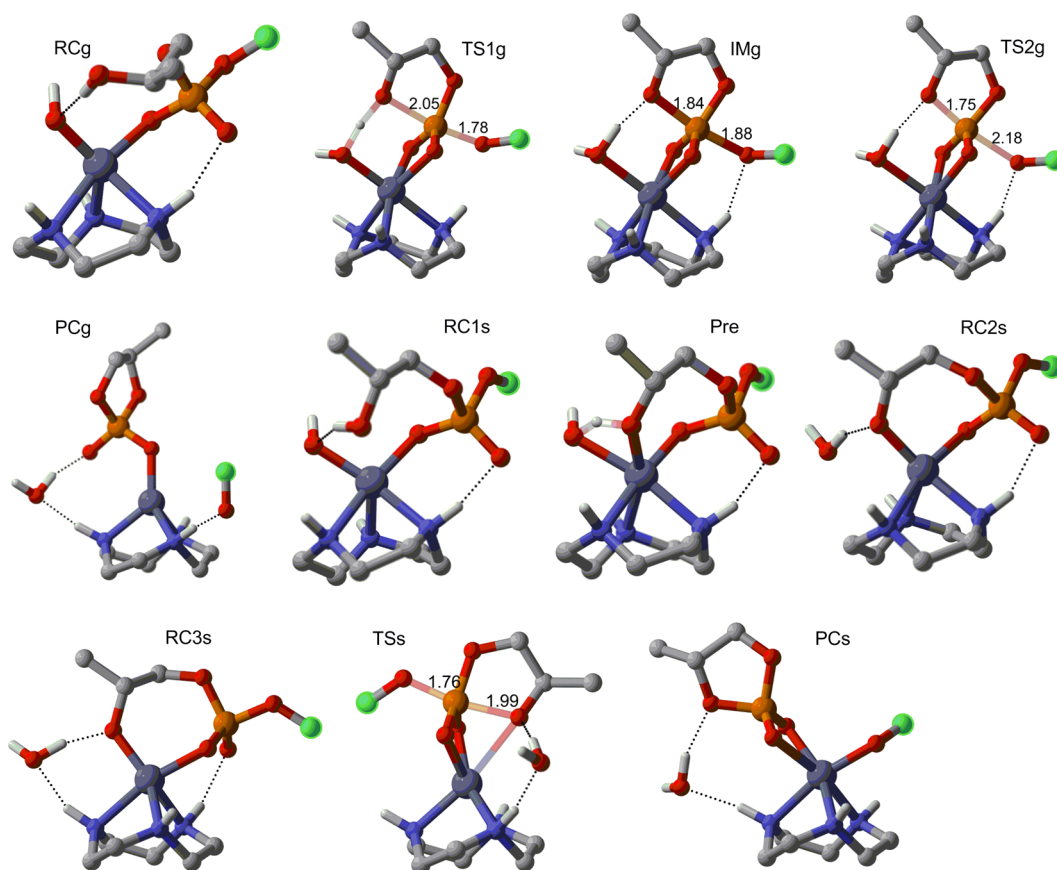


Figure 4. Optimized structures (in water) in the proposed mechanisms of the cyclization of HpPNP catalyzed by $\text{Zn}(\text{OH}):[9]\text{aneN}_3$. All carbon-bound hydrogen atoms and the leaving groups (linked to the highlighted carbon atom) are omitted for clarity. Key bond distances in the transition states are presented in angstroms.

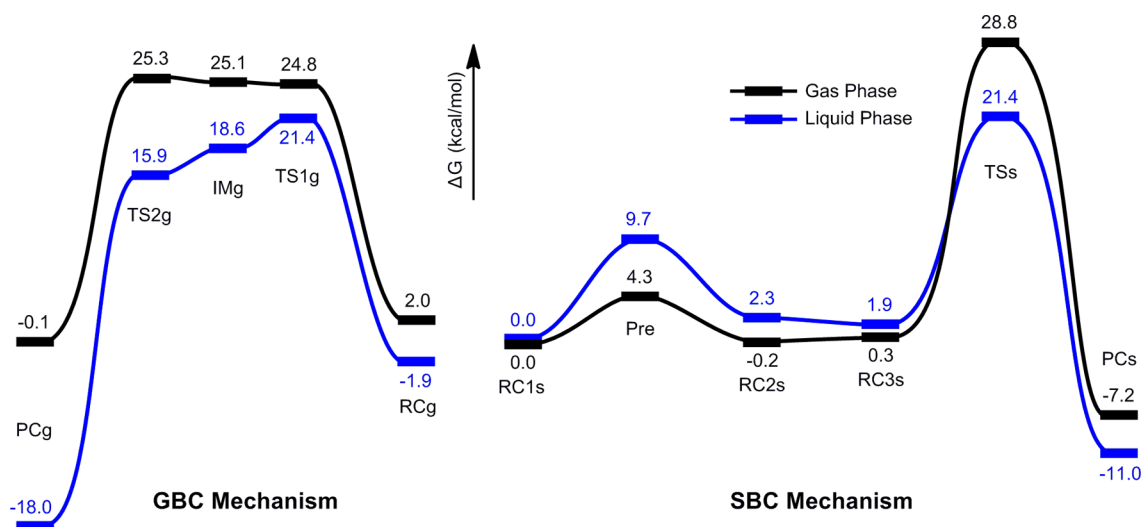


Figure 5. Relative free energy profiles of reaction structures (in water) in the proposed mechanisms of the cyclization of HpPNP catalyzed by $\text{Zn}(\text{OH}):[9]\text{aneN}_3$.

alcohols that the reaction is experimentally found to follow a GBC mechanism.^{15d,e,29} For metal-complex-promoted intramolecular HpPNP cyclization, the SBC mechanism cannot be occurring at the pH of the reaction because the amount of free alkoxide is too small to account for requisite deprotonation of the pendant hydroxypropyl group. However, the amount of free alkoxide cannot be manipulated in the current theoretical

approach, and the presupposed amount of metal-bound lyoxide is equivalent to the amount of the catalyst. The autoprotolysis of water is much easier than that of light alcohols, which implies that the amount of free hydroxide is distinctly larger than the alkoxide in the respective solvent. Therefore, the SBC mechanism is followed in aqueous solution, while the GBC mechanism is found in alcohols. The SBC mechanism could be

available in light alcohols or other reduced dielectric constant organic solvents in which a 0.5–1 equiv amount of free alkoxide is initially added in the solution.^{15f} Why do light alcohols, especially ethanol, impressively accelerate solvolysis cleavage of P–O bonds? Methanol and ethanol have structure and properties closet to water but have substantial lower dielectric constants ($\epsilon_s = 32.61, 24.85,$ and 78.35 for methanol, ethanol, and water, respectively). Reduced polarity solvents carry out important effects on the substantial rate acceleration by (1) enhancing electrostatic interactions between the positively charged catalyst and the negatively charged phosphate backbone of the substrate, (2) helping to better stabilize the charge-dispersed transition states and intermediates, and (3) increasing the solubility of metal complexes. Therefore, reduced polarity solvent media, such as light alcohols methanol and ethanol, are potent candidates for solvolysis cleavage of phosphate esters because of their significantly lower dielectric constant.

Mechanisms for the Cyclization of HpPNP Promoted by Zn(OH):[9]aneN₃ in Aqueous Solution. The proposed reaction pathways, optimized structures, and their relative free energy profiles determined are depicted in Scheme 4 and Figures 4 and 5, respectively. In reference to Zn:[12]aneN₃ issues, three pathways are proposed based on three different catalytic models, and among them, model B is the least favorable option. It should be noted that substantial efforts are made in our initial structural modeling in order to obtain the “favorable” models A and C, but only model B analogues are obtained. Further discussions are provided in ensuing chapters or paragraphs.

Two separate paths are obtained. As has been discussed above, mode 1-2 is more stable than mode 1-1, and thereby only mode 1-2 is considered in the issue. The GBC mechanisms in Zn:[12]aneN₃ issues are concerted, while that in the Zn:[9]aneN₃ system tends to be stepwise. Both proton transfer and nucleophilic attack are observed in the transition state TS1g. The P–O bond to the nucleophile is further strengthened in the subsequent phosphorane-like intermediate IMg. In IMg, the O(Nu)–P–O(LG) angle is 169.5° , and the P–O bond, to the nucleophile and leaving group (LG) are 1.84 and 1.88 Å, respectively. Then, the P–O bond to the leaving group is further cleaved in TS2g and finally broken in the transient product PCg. Both of the phosphoryl oxygen atoms are coordinated with the metal center in the high-energy species TS1g, IMg, and TS2g. Similarly, a SBC mechanism is also proposed, and proton transfer in the preequilibrium step and nucleophilic attack in the rate-limiting step are almost identical with their counterparts in the Zn:[12]aneN₃ system. It is worth noting that catalytic mode B is also adopted in the high-energy species TSs.

Inspection of Figure 5 shows that the energy differences between the GBC and SBC mechanisms are too small to be conclusive. The GBC mechanism in the Zn(OH):[9]aneN₃ system proceeds via intermediate IMg, which is midway in terms of the energy between TS1g and TS2g. Therefore, the lifetime of IMg is too short to exist, and IMg and TS1g are geometrically similar [both have a significant P–O(Nu) bond, while the P–O(LG) bond is slightly perturbed]. The gradient of the free energy versus reaction progress around TS1g is highly unsymmetrical, and thereby the GBC mechanism can be regarded as an enforced concerted process.³⁰ In reference to Figure 3, the lowest energy barrier of the cyclization of HpPNP catalyzed by Zn(OH):[12]aneN₃ is 15.4 kcal/mol, which is 6.0

kcal/mol lower than that in its reduced-sized counterpart Zn(OH):[9]aneN₃. Therefore, we can conclude that Zn:[12]aneN₃ is catalytically more favorable than Zn:[9]aneN₃ because of a lower energy barrier and, more importantly, a significant mechanistic preference to the SBC mechanism.

Why does the increasing size catalyst provide a lower energy barrier? The significant catalytic power diversities can be ascribed to the angles of N–Zn–N in the complexes (represented in Table 2). Inspection of Table 2 shows that

Table 2. Selected Structural Data from DFT-Calculated Transition States for the Cyclization of HpPNP Catalyzed by Zn(OH):[12]aneN₃ and Zn(OH):[9]aneN₃, Respectively

term ^a	1-TS	2-TS	3-TS	TS1g	TSs
N1–Zn–N2 ^b	92.0	90.4	103.8	79.4	82.0
N2–Zn–N3	91.7	90.4	102.7	79.2	84.0
N3–Zn–N1	105.2	101.1	105.9	80.8	81.9
N1–N2–N3–Zn ^c	57.8	57.8	43.8	62.3	58.9

^aN1, N2, and N3 refer to the nitrogen atoms in the catalyst. ^bThe angle of N1–Zn–N2 in degrees. ^cThe dihedral angle of N1–N2–N3–Zn in degrees.

the angles of N–Zn–N in the Zn(OH):[12]aneN₃ system (1-TS, 2-TS, and 3-TS) are larger than those in the Zn(OH):[9]aneN₃ system (TS1g and TSs). Meanwhile, the N–Zn–N angle in 3-TS is the largest among the five obtained transition states, which further leads to the smallest dihedral angle of N1–N2–N3–Zn and the resultant lowest energy barrier. The larger N–Zn–N angles (or the smaller N1–N2–N3–Zn dihedral angle) are favorable of a pentacoordinated configuration of the zinc(II) center and then lead to more space for the cis-oriented labile sites and, more importantly, can better stabilize the transition states, which are beneficial for reducing the energy barriers. For the Zn(OH):[9]aneN₃ system, the small N–Zn–N angles in combination with the large N1–N2–N3–Zn dihedral angle make the zinc(II) center significantly exposed to the solution, which are strongly in favor of a hexacoordinated configuration, and the catalytic mode B is favored. The strained P–O–Zn–O four-membered ring and the hexacoordinated zinc(II) center together make Zn:[9]aneN₃ catalytically inferior to Zn:[12]aneN₃. Our theoretical results are consistent with the experimental observations by Chin and co-workers¹⁷ that the increasing size ligands are beneficial to the catalytic power. The hexacoordinated configuration of zinc(II) centers is not very stable, which has been discussed in our previous works.^{19b,c} It should be noted that our computational results are not in agreement with the experimental findings reported in a previous paper by Mancin and collaborators,⁵ in which Zn:[9]aneN₃ turns out to be catalytically more powerful than Zn:[12]aneN₃. The difference in kinetic constants reported by Mancin and co-workers is 5-fold, which is much larger than any possible experimental error. The only answer is that the simplified model used in the present paper may not take into account all of the parameters affecting the reaction: first, participation of solvent molecules (interacting with the reaction complexes via hydrogen bonds and direct coordination linkages) during the reaction process, which cannot be perfectly solved by the presently utilized implicit solvent model; second, the different tendency to form unreactive μ -hydroxo dimers.^{26a} These unveiled parameters can be partly ascribed to the contradictory results obtained from experimental and theoretic-

cal works, and they clearly indicate the need for further investigations.

Characterization of Transition States. Key structural data of transition states are provided in Table 3. Inspection of

Table 3. Key Structural Data of Transition States for the Cyclization of HpPNP Catalyzed by Zn(OH):[12]aneN₃ and Zn(OH):[9]aneN₃, Respectively

term	1-TS	2-TS	3-TS	TS1g	TS2g	TSs
P–O(Nu) ^a	2.03	2.09	2.12	2.04	1.75	1.99
P–O(LG)	1.84	1.78	1.75	1.78	2.18	1.76
O(Nu)–P–O(LG) ^b	169.5	168.8	164.0	169.0	169.7	168.7
O2–O3–O4–P ^c	5.4	8.8	8.7	7.3	–12.6	7.5

^aThe P–O(Nu) bond length in angstroms. ^bThe angle of O(Nu)–P–O(LG) in degrees. ^cThe dihedral angle of O2–O3–O4–P in degrees. O2, O3, and O4 refer to the oxygen atoms in the equatorial plane of the phosphorane-like transition states.

Table 3 shows that the P–O(Nu) and P–O(LG) bond lengths, the O(Nu)–P–O(LG) angles, and the O2–O3–O4–P dihedral angles in 1-TS, 2-TS, 3-TS, TS1g, and TSs are close and the transition states locate more adjacent to the reactant than the product. By referring to the IRC results of paths 1 and 3 (Figure S1 in the SI), the IRC to the transition state (either 1-TS or 3-TS) and that from the transition state are unsymmetrical. The IRC to the reactant is sharp, while that to the product is blunt, which is consistent with the fact that the extent of P–O bond formation to the nucleophile is larger than that of P–O bond fission to the leaving group in the obtained transition states. The descending IRC to the product is not steady but with one or more slightly inclined “platforms”, which will be optimized to less stable intermediates if a lower-level basis set is used. This kind of phenomenon also exists in our previously reported works.^{19b,c} As demonstrated in Figure 5, the GBC mechanism in the Zn(OH):[9]aneN₃ system is a enforced concerted process rather than a stepwise pathway. Therefore, a conclusion can be made that concerted pathways are more preferable than the stepwise pathways in the mononuclear zinc(II)-complex-catalyzed reactions.

CONCLUSIONS

The cyclization of RNA dinucleotide analogue HpPNP promoted by mononuclear zinc(II) complexes is investigated in this paper by a theoretical approach. The coordination and binding modes of catalyst–substrate complexes are illustrated. The two cis-oriented labile coordination sites are preferred to coordinate with a substrate and a hydroxide ion. The hydrogen bonds between the catalyst and substrate play important roles in recognizing and stabilizing the substrate, and the most favorable pattern is that one N–H...O(P) hydrogen bond helps to stabilize the phosphate, while the other one N–H...O(Nu) hydrogen bond helps to bring the nucleophile into close proximity with the phosphorus center.

The ligand effect is discussed via a comparison of the mechanistic differences between the Zn(OH):[12]aneN₃ and Zn(OH):[9]aneN₃ systems. Three pathways are proposed when the cyclization of HpPNP is promoted by the Zn(OH):[12]aneN₃ complex. Paths 1 and 2 are GBC mechanisms in which both proton transfer and nucleophilic attack occur in the rate-limiting steps. Path 3 is a SBC mechanism in which proton transfer from the pendant hydroxypropyl group to the metal-

coordinated hydroxide ion occurs in the preequilibrium step, and only nucleophilic attack takes place in the rate-determining step. The energy barrier of path 3 is 15.4 kcal/mol and is the lowest one among the three proposed mechanisms, and thereby the SBC mechanism is more favorable in the Zn(OH):[12]aneN₃ system. Meanwhile, two pathways are proposed when using the Zn(OH):[9]aneN₃ complex. The energy barriers of the GBC and SBC mechanisms in the reduced size issue are very close and higher than that in path 3. Zn(OH):[12]aneN₃ is a better catalyst for a lower energetic barrier and the significant mechanistic preference to the SBC mechanisms. The great catalytic power of Zn(OH):[12]aneN₃ is thought to be ascribed to the large N–Zn–N angles in the complexes.

The solvent medium effect is also explored by involving water, methanol, and ethanol. The reaction coordinates are not changed and the values of the energy barriers are varied with a change of the solvent medium. The SBC mechanisms are relatively more favorable than the GBC mechanisms, and the energy barriers decrease with descending dielectric constant of the solvent medium. The reduced polarity/dielectric constant solvent media, such as methanol and ethanol, are potent candidates for catalyzed cleavage of the P–O bond of phosphate esters.

The debate of whether the reaction path is concerted or stepwise is also provided in the paper, and the results shows that concerted mechanisms are more preferable when promoted by mononuclear zinc(II) complexes.

Our theoretical observations are consistent with and, more importantly, systematically interpret the experimental results. The ligand and solvent medium effects are quite essential to the arrangement of the reaction conditions and catalyst design.

ASSOCIATED CONTENT

Supporting Information

Selected structural data of the optimized reaction structures in the proposed mechanisms, comparisons of the calculated results obtained from the B3LYP and BHandHLYP functionals, and total energy along the IRC in paths 1 and 3. This material is available free of charge via the Internet at <http://pubs.acs.org>.

AUTHOR INFORMATION

Corresponding Author

*E-mail: ceszhcy@mail.sysu.edu.cn. Fax: (+86) 84110523.

Notes

The authors declare no competing financial interest.

ACKNOWLEDGMENTS

We gratefully acknowledge the National Natural Science Foundation of China (Grants 21173273, 21373277, and J1103305) and Guangdong Provincial Natural Science Foundation (Grant 9351027501000003) for financial support. The research is also partially supported by the high-performance grid computing platform of Sun Yat-Sen University, Guangdong Province Key Laboratory of Computational Science, and Guangdong Province Computational Science Innovative Research Team. We sincerely thank the reviewers for their careful review and instructive comments of this manuscript.

REFERENCES

- (1) Westheimer, F. H. *Science* **1987**, *235*, 1173.

- (2) (a) Lipscomb, W. N.; Sträter, N. *Chem. Rev.* **1996**, *96*, 2375. (b) Wilcox, D. E. *Chem. Rev.* **1996**, *96*, 2435. (c) Hegg, E. L.; Burstyn, J. N. *Coord. Chem. Rev.* **1998**, *173*, 133. (d) Bashkin, J. K. *Curr. Opin. Chem. Biol.* **1999**, *3*, 752. (e) Krämer, R. *Coord. Chem. Rev.* **1999**, *182*, 243. (f) Kimura, E. *Curr. Opin. Chem. Biol.* **2000**, *4*, 207. (g) Kimura, E.; Kikuta, E. *J. Biol. Inorg. Chem.* **2000**, *5*, 139. (h) Molenveld, P.; Engbersen, J. F. J.; Reinhoudt, D. N. *Chem. Soc. Rev.* **2000**, *29*, 75. (i) Franklin, S. J. *Curr. Opin. Chem. Biol.* **2001**, *5*, 201. (j) Jackson, M. D.; Denu, J. M. *Chem. Rev.* **2001**, *101*, 2313. (k) O'Brien, P. J.; Herschlag, D. *Biochemistry* **2002**, *41*, 3207. (l) Liu, C.; Wang, M.; Zhang, T.; Sun, H. *Coord. Chem. Rev.* **2004**, *248*, 147. (m) Weston, J. *Chem. Rev.* **2005**, *105*, 2151. (n) Cleland, W. W.; Hengge, A. C. *Chem. Rev.* **2006**, *106*, 3252. (o) Niittymäki, T.; Lonngberg, H. *Org. Biomol. Chem.* **2006**, *4*, 15. (p) Stivers, J. T.; Nagarajan, R. *Chem. Rev.* **2006**, *106*, 3443. (q) Kamerlin, S. C. L.; Wilkie, J. *Org. Biomol. Chem.* **2007**, *5*, 2098. (r) Lonngberg, H. *Org. Biomol. Chem.* **2011**, *9*, 1687. (s) Desbouis, D.; Troitsky, I. P.; Belousoff, M. J.; Spiccia, L.; Graham, B. *Coord. Chem. Rev.* **2012**, *256*, 897. (t) Kamerlin, S. C. L.; Sharma, P. K.; Prasad, R. B.; Warshel, A. Q. *Rev. Biophys.* **2013**, *46*, 1. (u) Korhonen, H.; Koivusalo, T.; Toivola, S.; Mikkola, S. *Org. Biomol. Chem.* **2013**, *11*, 8324. (v) Zhao, M.; Wang, H.-B.; Ji, L.-N.; Mao, Z.-W. *Chem. Soc. Rev.* **2013**, *42*, 8360. (w) Mancin, F.; Scrimin, P.; Tecilla, P.; Tonellato, U. *Chem. Commun.* **2005**, 2540. (x) Mancin, F.; Scrimin, P.; Tecilla, P. *Chem. Commun.* **2012**, *48*, 5545.
- (3) Radzicka, A.; Wolfenden, R. *Science* **1995**, *267*, 90.
- (4) Thompson, J. E.; Kutateladze, T. G.; Schuster, M. C.; Venegas, F. D.; Messmore, J. M.; Raines, R. T. *Biorg. Chem.* **1995**, *23*, 471.
- (5) Bonfá, L.; Gatos, M.; Mancin, F.; Tecilla, P.; Tonellato, U. *Inorg. Chem.* **2003**, *42*, 3943.
- (6) (a) Morrow, J. R.; Amyes, T. L.; Richard, J. P. *Acc. Chem. Res.* **2008**, *41*, 539. (b) Livieri, M.; Mancin, F.; Saielli, G.; Chin, J.; Tonellato, U. *Chem.—Eur. J.* **2007**, *13*, 2246. (c) Oivanen, M.; Kuusela, S.; Lönnberg, H. *Chem. Rev.* **1998**, *98*, 961. (d) Perreault, D. M.; Anslyn, E. V. *Angew. Chem., Int. Ed. Engl.* **1997**, *36*, 432. (e) Gao, H.; Ke, Z.; DeYonker, N. J.; Wang, J.; Xu, H.; Mao, Z.-W.; Phillips, D. L.; Zhao, C. *J. Am. Chem. Soc.* **2011**, *133*, 2904. (f) Feng, G.; Mareque-Rivas, J. C.; Torres Martín de Rosales, R.; Williams, N. H. *J. Am. Chem. Soc.* **2005**, *127*, 13470. (g) Fan, Y.; Gao, Y. Q. *J. Am. Chem. Soc.* **2007**, *129*, 905. (h) Yang, M.-Y.; Iranzo, O.; Richard, J. P.; Morrow, J. R. *J. Am. Chem. Soc.* **2005**, *127*, 1064. (i) Maxwell, C. I.; Mosey, N. J.; Brown, R. S. *J. Am. Chem. Soc.* **2013**, *135*, 17209.
- (7) (a) Fritsky, I. O.; Ott, R.; Pritzkow, H.; Krämer, R. *Chem.—Eur. J.* **2001**, *7*, 1221. (b) Molenveld, P.; Engbersen, J. F. J.; Kooijman, H.; Spek, A. L.; Reinhoudt, D. N. *J. Am. Chem. Soc.* **1998**, *120*, 6726. (c) Liu, S.; Hamilton, A. D. *Tetrahedron Lett.* **1997**, *38*, 1107.
- (8) Deal, K. A.; Hengge, A. C.; Burstyn, J. N. *J. Am. Chem. Soc.* **1996**, *118*, 1713.
- (9) *Advances in Physical Organic Chemistry*; Gold, V., Ed.; Academic Press: New York, 1967.
- (10) (a) Iranzo, O.; Kovalevsky, A. Y.; Morrow, J. R.; Richard, J. P. *J. Am. Chem. Soc.* **2003**, *125*, 1988. (b) Mathews, R. A.; Rossiter, C. S.; Morrow, J. R.; Richard, J. P. *Dalton Trans.* **2007**, 3804. (c) O'Donoghue, A.; Pyun, S. Y.; Yang, M. Y.; Morrow, J. R.; Richard, J. P. *J. Am. Chem. Soc.* **2006**, *128*, 1615.
- (11) (a) Humphry, T.; Forconi, M.; Williams, N. H.; Hengge, A. C. *J. Am. Chem. Soc.* **2002**, *124*, 14860. (b) Williams, N. H.; Cheung, W.; Chin, J. *J. Am. Chem. Soc.* **1998**, *120*, 8079.
- (12) Liu, C. T.; Neverov, A. A.; Brown, R. S. *J. Am. Chem. Soc.* **2008**, *130*, 13870.
- (13) Bonomi, R.; Saielli, G.; Scrimin, P.; Mancin, F. *Supramol. Chem.* **2013**, *25*, 665.
- (14) Richard, J. P.; Amyes, T. L. *Biorg. Chem.* **2004**, *32*, 354.
- (15) (a) Bunn, S. E.; Liu, C. T.; Lu, Z.-L.; Neverov, A. A.; Brown, R. S. *J. Am. Chem. Soc.* **2007**, *129*, 16238. (b) Lu, Z.-L.; Liu, T.; Neverov, A. A.; Brown, R. S. *J. Am. Chem. Soc.* **2007**, *129*, 11642. (c) Neverov, A. A.; Lu, Z.-L.; Maxwell, C. I.; Mohamed, M. F.; White, C. J.; Tsang, J. S. W.; Brown, R. S. *J. Am. Chem. Soc.* **2006**, *128*, 16398. (d) Liu, C. T.; Neverov, A. A.; Brown, R. S. *J. Am. Chem. Soc.* **2008**, *130*, 16711. (e) Brown, R. S.; Lu, Z.-L.; Liu, C. T.; Tsang, W. Y.; Edwards, D. R.; Neverov, A. A. *J. Phys. Org. Chem.* **2010**, *23*, 1. (f) Liu, C. T.; Neverov, A. A.; Brown, R. S. *Inorg. Chem.* **2007**, *46*, 1778.
- (16) Koike, T.; Kimura, E. *J. Am. Chem. Soc.* **1991**, *113*, 8935.
- (17) (a) Chin, J.; Banaszczyk, M.; Jubian, V.; Zou, X. *J. Am. Chem. Soc.* **1989**, *111*, 186. (b) Chin, J.; Zou, X. *J. Am. Chem. Soc.* **1988**, *110*, 223.
- (18) Frisch, M. J.; Trucks, G. W.; Schlegel, H. B.; Scuseria, G. E.; Robb, M. A.; Cheeseman, J. R.; Scalmani, G.; Barone, V.; Mennucci, B.; Petersson, G. A.; Nakatsuji, H.; Caricato, M.; Li, X.; Hratchian, H. P.; Izmaylov, A. F.; Bloino, J.; Zheng, G.; Sonnenberg, J. L.; Hada, M.; Ehara, M.; Toyota, K.; Fukuda, R.; Hasegawa, J.; Ishida, M.; Nakajima, T.; Honda, Y.; Kitao, O.; Nakai, H.; Vreven, T.; Montgomery, J. A., Jr.; Peralta, J. E.; Ogliaro, F.; Bearpark, M.; Heyd, J. J.; Brothers, E.; Kudin, K. N.; Staroverov, V. N.; Kobayashi, R.; Normand, J.; Raghavachari, K.; Rendell, A.; Burant, J. C.; Iyengar, S. S.; Tomasi, J.; Cossi, M.; Rega, N.; Millam, M. J.; Klene, M.; Knox, J. E.; Cross, J. B.; Bakken, V.; Adamo, C.; Jaramillo, J.; Gomperts, R.; Stratmann, R. E.; Yazyev, O.; Austin, A. J.; Cammi, R.; Pomelli, C.; Ochterski, J. W.; Martin, R. L.; Morokuma, K.; Zakrzewski, V. G.; Voth, G. A.; Salvador, P.; Dannenberg, J. J.; Dapprich, S.; Daniels, A. D.; Farkas, Ö.; Foresman, J. B.; Ortiz, J. V.; Cioslowski, J.; Fox, D. J. *Gaussian 09*, revision A.01; Gaussian, Inc.: Wallingford, CT, 2009.
- (19) (a) Zhang, X.; Gao, H.; Xu, H.; Xu, J.; Chao, H.; Zhao, C. *J. Mol. Catal. A: Chem.* **2013**, *368–369*, 53. (b) Zhang, X.; Xu, X.; Xu, H.; Zhang, X.; Phillips, D. L.; Zhao, C. *ChemPhysChem* **2014**, *15*, 1887. (c) Zhang, X.; Zhu, Y.; Zheng, X.; Phillips, D. L.; Zhao, C. *Inorg. Chem.* **2014**, *53*, 3354.
- (20) (a) Becke, A. D. *J. Chem. Phys.* **1993**, *98*, 5648. (b) Lee, C. Y. W.; Parr, R. G. *Phys. Rev. B* **1988**, *37*, 785.
- (21) Becke, A. D. *J. Chem. Phys.* **1993**, *98*, 1372.
- (22) Dolg, M.; Wedig, U.; Stoll, H.; Preuss, H. *J. Chem. Phys.* **1987**, *86*, 866.
- (23) Fukui, K. *Acc. Chem. Res.* **1981**, *14*, 363.
- (24) Cossi, M.; Scalmani, G.; Rega, N.; Barone, V. *J. Chem. Phys.* **2002**, *117*, 43.
- (25) Marenich, A. V.; Cramer, C. J.; Truhlar, D. G. *J. Phys. Chem. B* **2009**, *113*, 6378.
- (26) (a) Hegg, E. L.; Mortimore, S. H.; Cheung, C. L.; Huyett, J. E.; Powell, D. R.; Burstyn, J. N. *Inorg. Chem.* **1999**, *38*, 2961. (b) Mohamed, M. F.; Sanchez-Lombardo, I.; Neverov, A. A.; Brown, R. S. *Org. Biomol. Chem.* **2012**, *10*, 631.
- (27) Desloges, W.; Neverov, A. A.; Brown, R. S. *Inorg. Chem.* **2004**, *43*, 6752.
- (28) (a) Kimura, E.; Nakamura, I.; Koike, T.; Shionoya, M.; Kodama, Y.; Ikeda, T.; Shiro, M. *J. Am. Chem. Soc.* **1994**, *116*, 4764. (b) Young, M. J.; Wahnon, D.; Hynes, R. C.; Chin, J. *J. Am. Chem. Soc.* **1995**, *117*, 9441.
- (29) Sánchez-Lombardo, I.; Yatsimirsky, A. K. *Inorg. Chem.* **2008**, *47*, 2514.
- (30) IUPAC. *Compendium of Chemical Terminology*, 2nd ed. (the "Gold Book"); compiled by McNaught, A. D.; Wilkinson, A. Blackwell Scientific Publications: Oxford, U.K., 1997. XML online-corrected version: <http://goldbook.iupac.org>, 2006.